ELSEVIER

Journal of Organometallic Chemistry 573 (1999) 156–164

Journal of Organometallic Chemistry

Synthesis of mixed-metal Li/M, M/M′ and mixed valence M^{I}/M^{III} chelate amido complexes of the heavy Group 13 metals (M = In, Tl)[1]

Konrad W. Hellmann [a], Annina Bergner [a], Lutz H. Gade [a,*], Ian J. Scowen [b], Mary McPartlin [b]

[a] *Institut für Anorganische Chemie and Institut für Organische Chemie der Universität Würzburg, Am Hubland, 97074 Würzburg, Germany*
[b] *School of Applied Chemistry, University of North London, Holloway Road, London N7 8DB, UK*

Abstract

Reaction of the difunctional lithium amide $[H_2C\{CH_2N(Li)SiMe_3\}_2]_2$ (**2**) or its ether adduct $[H_2C\{CH_2N(Li–THF)SiMe_3\}_2]$ (**3**) with MCl_3 (M = In, Ga, Tl) gave the mixed metal amides $[\{CH_2(CH_2NSiMe_3)_2\}_2M–Li(THF)_2]$ (M = In: **4**, Ga: **5**, Tl: **6**) which are highly fluctional in solution. Metal exchange of the thallium(I) amide with MCl_3 yielded the mixed-metal/valent species $[\{CH_2(CH_2NSiMe_3)_2\}_2M^{III}Tl^{I}]$ (M = In: **7**, Tl: **8**) both of which were characterized by X-ray crystallography and found to have the trivalent metal at the centre of a distorted tetrahedral coordination sphere of the amide donors while the monovalent Tl atom bridges two such donor functions.

Keywords: Difunctional lithium amide; Mixed metal amides; Metal Exchange; Distorted tetrahedral coordination sphere

1. Introduction

The chemistry of the low valent heavy Group 13 element amides is dominated by redox disproportionations in solution and the formation of either mixed-valent species or completely demetallated products [1,2]. This aspect of their chemistry has been the limiting factor in our investigation into the forms of aggregation displayed by In^{I} and Tl^{I} amides in the solid [3,4]. For thallium amides these are defined by the van der Waals attraction between the heavy metal atoms, generating finite or infinite supramolecular motifs in their crystal structures [5,6].

The unusual double-stranded chain structure of the thallium amide $[CH_2\{CH_2N(Tl)SiMe_3\}_2]_\infty$ (**1**) established by its crystal structure (Scheme 1) [4] prompted us to investigate more closely the chemistry of the heavy Group 13 amides containing the chelating amido ligand $[CH_2\{CH_2NSiMe_3\}_2]^{2-}$ [7,8].

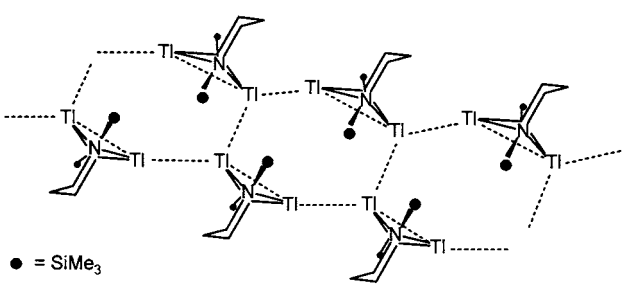

Scheme 1. Aggregation of $[CH_2\{CH_2N(Tl)SiMe_3\}_2]_\infty$ (**1**) in the crystal.

2. Results and discussion

2.1. Synthesis and crystal structure of the lithium amide $[H_2C\{CH_2N(Li)SiMe_3\}_2]_2$ (2)

As ligand transfer reagent we chose the lithium amide $[H_2C\{CH_2N(Li)SiMe_3\}_2]_2$ (**2**) which was generated from the diamine precursor by reaction with two molar equivalents of *n*-butyllithium in a non-coordinating hydrocarbon solvent:

* Corresponding author. Fax: +49 931 8884605; e-mail: lutz.gade@mail.uni-wuerzburg.de

[1] Dedicated to Professor Brian Johnson, colleague and friend, on the occasion of his 60th birthday.

0022-328X/99/$ - see front matter
PII S0022-328X(98)00652-4

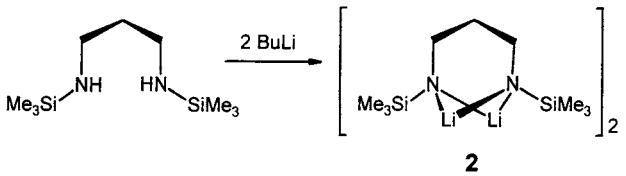

2

Cryoscopic measurements performed in benzene indicated a dimeric lithium amide aggregate in this solvent. In order to establish its structure in the solid state a single crystal X-ray structure analysis of **2** was carried out. This confirmed its dimeric structure, the centre piece being a heterocubane array of the Li- and N-atoms (Fig. 1, Table 1). The central $(LiN)_4$-cube is distorted due to the influence of the bridging propylene unit in the chelate rings which limits the structural degrees of freedom of the amido-N atoms.

The Li–N distances lie in the range of 2.04–2.09 Å which is in accord with previously established structures of amidolithium compounds. The overall structural pattern is closely related to that of several difunctional lithium-amides such as $[\{^tBuN(Li)\}_2SiMe_2]_2$ and $[Li\{rac\text{-}N(^tBu)CH(Me)CH(Me)N^tBu\}Li]_2$ published, respectively, by Bürger [9] and more recently Raston and coworkers [10]. The driving force of the dimerization is the maximization of the Li–N bond connectivity, in other words, the electrostatic attraction between the positive charged Li-cations and the amido-anions. Within this ionic interpretation of the Li–N-structure the hypercoordination (coordination number 5) at the amido-N-atom is not unexpected [11].

Since the metal exchange reactions are being carried out in ether solvents the THF-adduct of **2** was gener-

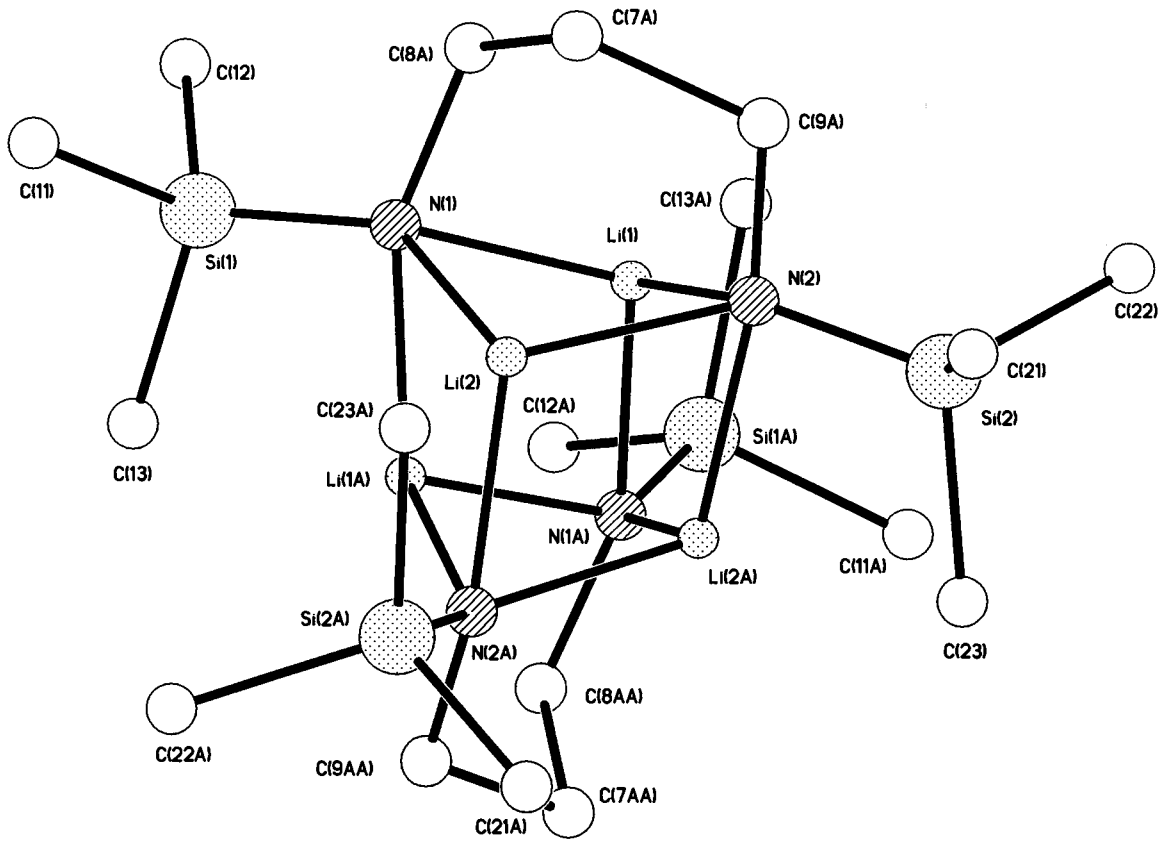

Fig. 1. Molecular structure of **2**. Selected bond lengths (Å) and interbond angles (°) are shown in Table 1.

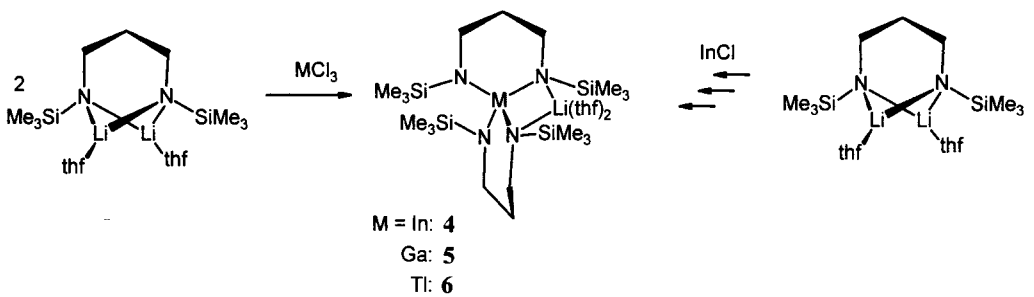

Scheme 2. Synthesis of complexes **4**–**6**.

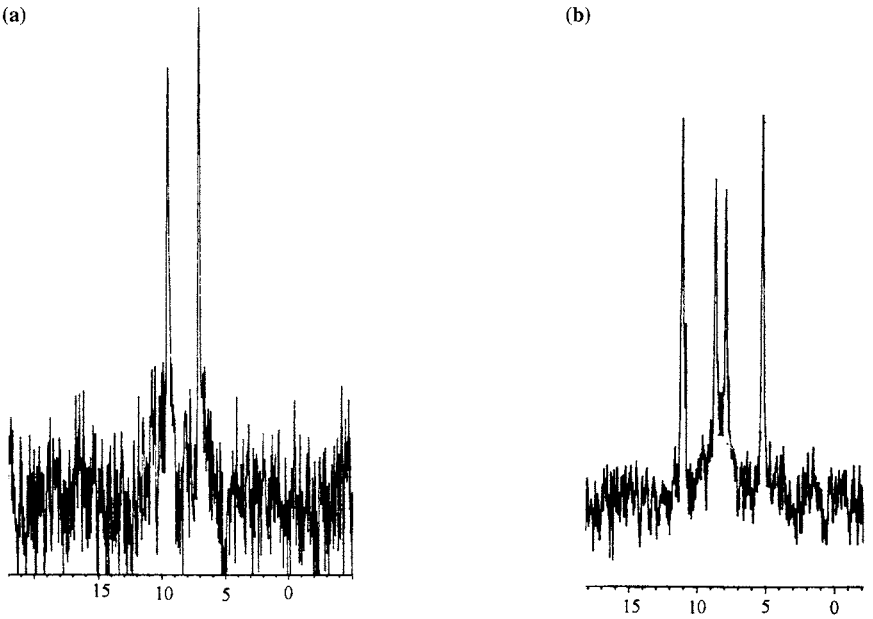

Fig. 2. ^{29}Si-NMR spectra of **6** recorded in toluene-d_8 at 310 K (a) and at 220 K (b) displaying $^{203/205}$Tl–^{29}Si-coupling.

ated and isolated as a colourless crystalline solid. On the basis of its analytical and spectroscopic data it is formulated as $[H_2C\{CH_2N(Li–THF)SiMe_3\}_2]$ (**3**).

2.2. Metal exchange reactions with MCl and MCl_3 (M = In, Tl)

In view of the straightforward synthesis of $[CH_2\{CH_2N(Tl)SiMe_3\}_2]_\infty$ (**1**) and its remarkable crystal structure, we were interested in the homologous compound of indium(I) and its properties. It was thought that this would provide additional insight into the importance which the heavy metal–metal-interactions in the thallium compound have in determining its crystal structure.

Upon addition of InCl to a solution of **3** in THF, an immediate redox disproportion took place as evidenced by the precipitation of indium metal. From the resulting product mixture, after work up, a yellow, microcrystalline compound could be isolated in low yield. Based on its analytical as well as ^{1}H-, ^{13}C-, ^{7}Li and ^{29}Si-NMR spectroscopic data we formulated the product as a mixed metal Li/In^{III}-amide $[\{CH_2(CH_2NSiMe_3)_2\}_2InLi(THF)_2]$ (**4**) which is thought to be structurally related to the mixed indium(III)-lithium amide $[\{Me_2Si(NSiMe_3)_2\}_2In$-Li] reported recently by Veith and coworkers [12]. Compound **4** as well as its gallium and thallium analogues, **5** and **6**, can be synthesized directly and in high yield by reaction of the lithium amide **3** with the metal trihalides MCl_3 (Scheme 2).

The NMR-spectroscopic investigation of all three compounds uncovered a remarkable dynamic behaviour which was studied at variable temperatures. The ^{1}H-, ^{13}C- and ^{29}Si-NMR spectra of $[\{CH_2(CH_2NSiMe_3)_2\}_2GaLi(THF)_2]$ (**5**) recorded in toluene-d_6 at 295 K are consistent with a molecular D_{2d} symmetry on the timescale of the experiment. Only one singlet resonance is observed for the Me_3Si-groups in the ^{1}H-NMR spectrum at $\delta = 0.38$ as well as two multiplets assigned to the central and N-bonded methylene groups of the chelate rings centred at, respectively, 1.75 and 3.21 ppm. The observation of only three signals for the amide unit in the ^{13}C-NMR spectrum is equally consistent with an effective molecular symmetry which is higher than that formulated in Scheme 2. In order to study the dynamic processes the ^{29}Si-nuclei present in the molecule proved to be the ideal probes. At 295 K a single resonance is observed at $\delta = 5.6$ which is broadened upon cooling the sample. Coalescence is reached at 275 K below which two resonances appear which sharpened up at 215 K ($\delta = 5.0$ and 6.0) and indicate the reduction of the effective symmetry as the fluctional process is 'frozen out'. The overall dynamic process which is characterized by a free activation enthalpy of 53.2($\pm$0.5) kJ mol^{-1} [13].

The observed fluctionality and its manifestation in the variable temperature NMR-spectra may be explained by the 'rotation' of the $[Li(THF)_2]^+$-ion around the 'amido-belt' of the tetraamidogallate unit, which may occur either by a non-dissociative or a dissociative mechanism. However, in case of the latter, the cationic fragment is thought to remain within the solvent cage of the molecule. This dynamic process is closely related to the dynamics of the non-solvated lithium bis-(chelateamido)indate $[\{Me_2Si(NSiMe_3)_2\}_2InLi]$ reported by Veith and coworkers, for which an activation barrier of 44.3 kJ mol^{-1} was determined [12].

The analogous dynamic rearrangements in the indium(III) and thallium(III) compounds **4** and **6** occur with

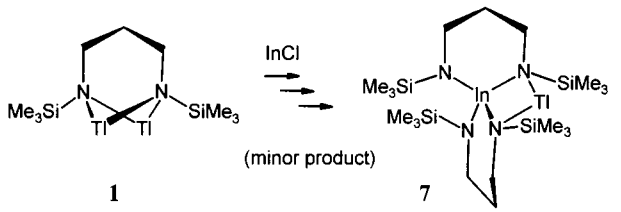

Scheme 3. Isolation of **7** in low yield from the attempted metal exchange of **1** with InCl.

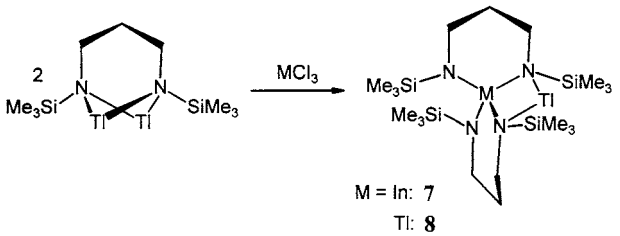

Scheme 4. Rational synthesis of **7** and **8**.

an activation barrier which is identical to that of **5** within experimental error (**4**: 54.7($\pm$0.5) kJ mol^{-1}; **6**: 54.1($\pm$0.5) kJ mol^{-1} determined by ^{29}Si-NMR spectroscopy) [13]. An interesting feature of the ^{29}Si-NMR spectra of the thallium compound **6** is the coupling with the $^{203/205}$Tl nuclei. As a consequence, the resonance in the ^{1}H-NMR spectrum recorded at 295 K of the inner CH_2-group in the propylene bridge appears as a doublet of quintets at $\delta = 1.73$ with a $^{4}J_{TlH}$ of 43 Hz, while the signals assigned to the CH_2 groups adjacent to the amido-N functions at $\delta = 3.49$ are split by 316 Hz due to $^{3}J_{TlH}$-coupling.

The ^{29}Si-NMR signal attributed to the trimethylsilyl groups in the thallium compound **6** appears as a doublet at 310 K (Fig. 2a) with an average $^{2}J_{TlSi}$ of 100.3 Hz. The different thallium-silicon coupling constants expected for the two resonances, which in the low temperature limit represent the static structure of **6**, are observed at 220 K: a doublet at $\delta = 8.1$ [$^{2}J_{TlSi}$ = 232.0 Hz] and a second doublet-'inscribed' in the first-at $\delta = 8.3$ [$^{2}J_{TlSi} = 30.2$ Hz] (Fig. 2b). The considerable difference of the coupling constants is due to the influence of the bridging {Li(THF)$_2$}-unit which upon binding to two of the four amido-N atoms, changes the geometric parameters which determine the magnitude of the coupling. Although an unambiguous assignment of the two ^{29}Si-NMR resonances based on this reasoning is not possible, we would like to point out that in the crystal structures of the mixed valent M^{I}M^{III}-amides discussed below the tetracoordination at the two M^{I}-bridged N-functions leads to a lengthening of the metal(III)-N bonds. This in turn would reduce the Tl-Si coupling observed for the $SiMe_3$-groups attached to these nitrogen atoms so that, by implication, we tentatively assign the ^{29}Si-NMR signal with the small coupling contant at δ = 8.3 to these trimethylsilyl groups.

2.3. Tl-Tl and Tl-In exchange reactions: synthesis and structural characterization of dinuclear mixed-valent and mixed-metal amides

The isolation of the bis-chelate **4** was the result of an attempt to synthesize the In^{I}-amide corresponding to the thallium 'polymer' **1**. The latter itself may act as an amide transfer reagent as observed in reactions with transition metal halides and we therefore reacted **1** with two molar equivalents of InCl in THF. After addition of the solid indium(I) chloride at -78°C the reaction mixture was warmed to room temperature (r.t.) resulting in the precipitation of indium and varying small quantities of thallium metal (as established by elemental analysis) as well as a yellow supernatent solution. From this a yellow crystalline compound was isolated in ca. 30% yield which was formulated as [{CH_2(CH_2N$SiMe_3$)$_2$}$_2$InTl] (**7**) on the basis of its analytical and NMR-spectroscopic data (including a metal analysis). In view of the greater stability of the monovalent oxidation state for thallium in comparison to indium, this mixed metal species was formulated as an In^{III}Tl^{I}-complex as shown in Scheme 3.

While this was an ad hoc assumption, a single crystal X-ray structure analysis established its identity and detailed structural arrangement. The indium and thallium atoms in the dinuclear complex **7** are part of a tricyclic structure consisting of the two six-membered chelate rings and the adjacent four-membered dimetallacycle (Fig. 3, Table 2).

The expected tetrahedral coordination geometry of the tetraamidoindate(III) is significantly distorted by the bridging Tl^{I}-atom. Apart from the resulting wide variation of the N–In–N interbond angles [N(2)–In(1)–N(4) 122.7(8), N(2)–In(1)–N(3) 116.8(8), N(4)–In(1)–N(3) 98.7(7), N(2)–In(1)–N(1) 100.7(7), N(4)–In(1)–N(1) 119.2(9), N(3)–In(1)–N(1) 96.5(7)°] with the particularly acute thallium-bridged N(3)–In(1)–N(1) angle of 96.5(7)° the effect of the peripheral Tl^{I}-binding is reflected in the increase of the In–N1 and In–N3 distances [2.208(14) and 2.207(14) Å, respectively] of ca. 0.2 Å in comparison to the In–N-bonds not affected by the coordination of the thallium cation.

After many attempts, satisfactory refinement of the structure of **7** was achieved with a model in which ca. 15% of the inverse Tl^{III}In^{I}-complex is randomly distributed in the crystal. While this observation is consistent with the detection of thallium in the metal

precipitate formed in the reaction, the crystalline compound only gave rise to one set of NMR signals when dissolved in C_6D_6 or toluene-d_8. At this stage we are not able to comment on this apparent discrepancy and the possibility of a mutual conversion of the two redox isomers in solution.

The compound could be obtained in better yield (65%) by direct synthesis from **1** and $InCl_3$ as confirmed by the identical analytical and spectroscopic data. Using the analogous route, reaction of **1** with $TlCl_3$ gave the mixed-valent $Tl^{I}Tl^{III}$-amide $[\{CH_2(CH_2NSiMe_3)_2\}_2Tl^{III}Tl^{I}]$ (**8**) (Scheme 4).

In order to establish the structure of **8** unambiguously an X-ray diffraction study was carried out which revealed that **7** and **8** are isomorphous, both forming orthorhombic crystals (space group *Pna*2) of closely similar unit cell dimensions, a finding which is not unexpected in view of the co-crystallization of the two redox-isomers of **7**. The overall molecular structure of the dithallium compound **8** in the solid state (Fig. 4, Table 3) is therefore virtually identical to that of **7**.

Unfortunately, due to very poor diffraction by both sets of crystals the S.D. of all parameters of **7** and **8** are relatively high, thus precluding detailed discussion of the bond lengths and angles. Both **7** and **8** display dynamic behaviour in solution as reflected in the NMR spectra recorded at variable temperature. In view of its greater thermal stability a variable temperature ^{29}Si-NMR study of **8** was carried out. The low temperature limit spectrum representing the static structure could be obtained at temperatures ≤ 220 K. The coupling pattern observed at 220 K is related to that of **6** discussed earlier in this paper and is depicted in Fig. 5.

The doublet resonance at $\delta = 8.2$ with the large $^2J(^{203/205}Tl-^{29}Si)$ coupling of 238 Hz is again assigned to the $SiMe_3$-groups at the N-donor which are not bridged by the Tl^{I}-atom. The second multiplet which appeared as a doublet in the low temperature spectrum of **6** is observed as an unresolved multiplet due to coupling to both the Tl^{III} and Tl^{I} nuclei. We have previously observed that coupling to monovalent thallium leads to considerable resonance broadening probably due to the rapid relaxation of the metal nucleus.

3. Experimental

All manipulations were performed under purified argon in standard (Schlenk) glassware which was flame dried with a Bunsen burner prior to use. Separation of solids from suspensions occurred by centrifugation only, all filtration procedures being avoided that way. The centrifuge employed was a Rotina 48 by Hettich Zentrifugen, Tuttlingen, Germany, which was equipped with a specially designed Schlenk-tube rotor [14]. Solvents were dried according to standard procedures. The deuterated solvents used for the NMR spectroscopic measurements were degassed by three successive 'freeze-pump-thaw' cycles and dried over 4-Å molecular sieves.

The ^{1}H- ^{13}C-, ^{29}Si- and ^{7}Li-NMR spectra were recorded on a Bruker AC 200 spectrometer equipped with a B-VT-2000 variable temperature unit (at 200.13, 50.32, 39.76 and 77.78 MHz, respectively) with tetramethylsilane and LiI (1 M in H_2O, ext.) as references. Elemental analyses were carried out in the microanalytical laboratory of the chemistry department at Würzburg.

3.1. Preparation of $\{CH_2[CH_2N(Li)SiMe_3]_2\}_2$ 2 and $CH_2[CH_2N(LiTHF)SiMe_3]_2$ 3

To a stirred solution of 2.00 g (9.15 mmol) $CH_2(CH_2NHSiMe_3)_2$ in 20 ml hexane (preparation for compound **2**) or THF (preparation of compound **3**) 7.32 ml (18.31 mmol) of a 2.5 M BuLi solution in hexane was added at -75°C. The mixture was allowed to react at r.t. for an additional hour. While removing the solvent in vacuo compounds **2** and **3** were precipitated as colourless, crystalline solids. Compound **3** was recrystallized from pentane.

Analytical data of compound **2**: Yield: 1.92 g (91%), (found: C, 46.99; H, 10.71; N, 12.04. $C_9H_{24}N_2Si_2Li_2$ calc.: C, 46.93; H, 10.50; N, 12.16). ^{1}H-NMR (200.13 MHz, C_6D_6, 295 K): δ 0.16 (s, 36 H, $Si(CH_3)_3$), 1.47 (m, 4 H, CH_2CH_2N), 3.17 (m, 8 H, CH_2N). ^{13}C-NMR (50.32 MHz, C_6D_6, 295 K): δ 0.2 ($Si(CH_3)_3$), 39.4 (CH_2CH_2N), 49.3 (CH_2N). ^{7}Li-NMR (77.77 MHz, C_6D_6, 295 K): δ 0.84.

Analytical data of compound **3**: Yield: 2.70 g (85%), (found: C, 58.62; H, 11.48; N, 7.91. $C_{17}H_{40}N_2Si_2Li_2O_2$ calc.: C, 58.75; H, 11.60; N, 8.06). ^{1}H-NMR (200.13 MHz, [d_6]-benzene, 295 K): δ 0.29 (s, 18 H, $Si(CH_3)_3$), 1.31 (m, 8 H, CH_2CH_2O), 1.84 (m, 2 H, CH_2CH_2N), 3.37 (m, 4 H, CH_2N), 3.53 (m, 8H, CH_2CH_2O). ^{13}C-NMR (50.32 MHz, [d_6]-benzene, 295 K): δ 2.1 ($Si(CH_3)_3$), 25.3 (CH_2CH_2O), 42.9 (CH_2CH_2N), 48.3 (CH_2NN), 68.6 (CH_2CH_2O). ^{7}Li-NMR (77.77 MHz, [d_6]-benzene, 295 K): δ 0.23. ^{29}Si-NMR (39.76 MHz, [d_6]-benzene, 295 K): δ 6.3.

3.2. Preparation of $\{[CH_2(CH_2NSiMe_3)_2]_2M\}Li(THF)_2$ ($M = In$ 4, Ga 5, Tl 6)

A stirred solution of 1.00 g (2.88 mmol) $CH_2[CH_2N(LiTHF)SiMe_3]_2$ **3** in 20 ml THF was allowed to react with 0.5 equivalents (1.44 mmol) of MCl_3 (M = In **4**, Ga **5**, Tl **6**) at -78°C. After warm-

Table 1
Selected bond lengths (Å) and interbond angles (°) of **2**

Bond lengths (Å)			
N(1)–Li(1)	2.040(8)	N(1)–Li(2)	2.053(8)
N(2)–Li(1)	2.048(8)	N(2)–Li(2)	2.044(8)
N(1)–Li(1′)	2.084(8)	N(2)–Li(2′)	2.090(8)
Si(1)–N(1)	1.714(3)	Si(2)–N(2)	1.710(3)
Bond angles (°)			
Li(1)–N(1)–Li(2)	75.6(3)	Li(1)–N(1)–Li(1′)	70.6(3)
Li(2)–N(1)–Li(1′)	70.2(3)	Li(2)–N(2)–Li(2′)	70.8(4)
N(1)–Li(1)–N(2)	98.2(3)	N(1)–Li(1)–N(1′)	108.0(3)
N(2)–Li(1)–N(1′)	109.0(4)	C(8A)–N(1)–Si(1)	110.2(4)
C(8A)–N(1)–Li(1)	83.9(4)	Li(1)–N(1)–Li(1)	135.2(3)
C(8A)–N(1)–Li(2)	102.0(4)	Si(1)–N(1)–Li(2)	136.4(3)
C(9A)–N(2)–Li(2)	105.6(4)	C(9A)–N(2)–Si(2)	105.7(4)
Si(2)–N(2)–Li(2)	134.6(3)	C(9A)–N(2)–Li(1)	88.7(5)

ing to r.t. the mixture was stirred for 20 h and the solvent removed in vacuo. The residue was extracted with pentane (10 ml) and unsoluable products removed by centrifugation. The solvent was removed yielding compounds **4**–**6** as colourless (**4** and **5**) or yellow (**6**) amorphous solids after drying for 6 h in high vacuum. On recrystallization in a small amount of pentane the analytically pure compounds **4**–**6** were obtained.

Analytical data for compound **4**: Yield: 1.27 g (63%), (found: C, 44.29; H, 8.98; N, 7.85; In 16.61. $C_{26}H_{64}LiInN_4O_2Si_4$ calc.: C, 44.68; H, 9.23; N, 8.02; In 16.43). ^{1}H-NMR (200.13 MHz, [d_6]-benzene, 295 K): δ 0.36 (s, 36 H, $Si(CH_3)_3$), 1.35 (m, 8 H, CH_2CH_2O), 1.72 (m, 4 H, CH_2CH_2N), 3.27 (m, 8 H, CH_2N), 3.29 (m, 8H, CH_2CH_2O). ^{13}C-NMR (50.32 MHz, C_6D_6, 295 K): δ 1.8 ($Si(CH_3)_3$), 25.6 (CH_2CH_2O), 41.0 (CH_2CH_2N), 49.2 (CH_2NN), 68.8 (CH_2CH_2O). ^{7}Li-NMR (77.77 MHz, [d_6]-benzene, 295 K): δ 1.59. ^{29}Si-NMR (39.76 MHz, C_6D_6, 295 K): δ 6.9.

Analytical data for compound **5**: Yield: 1.54 g (82%), (found: C, 47.34; H, 9.56; N, 8.29. $C_{26}H_{64}GaLiN_4O_2Si_4$ calc.: C, 47.76; H, 9.87; N, 8.57). ^{1}H-NMR (200.13 MHz, [d_6]-benzene, 295 K): δ 0.38 (s, 36 H, $Si(CH_3)_3$), 1.26 (m, 8 H, CH_2CH_2O), 1.75 (m, 4 H, CH_2CH_2N), 3.21 (m, 8 H, CH_2N), 3.35 (m, 8H, CH_2CH_2O). ^{13}C-NMR (50.32 MHz, [d_6]-benzene, 295 K): δ 1.9 ($Si(CH_3)_3$), 25.4 (CH_2CH_2O), 36.8 (CH_2CH_2N), 47.0 (CH_2NN), 68.1 (CH_2CH_2O). ^{7}Li-NMR (77.77 MHz, C_6D_6, 295 K): δ 3.19. ^{29}Si-NMR (39.76 MHz, [d_6]-benzene, 295 K): δ 5.6.

Analytical data for compound **6**: Yield: 1.77 g (84%), (found: C, 39.21; H, 7.99; N, 6.82; Tl 25.87. $C_{26}H_{64}LiN_4O_2Si_4Tl$ calc.: C, 39.61; H, 8.18; N, 7.11;

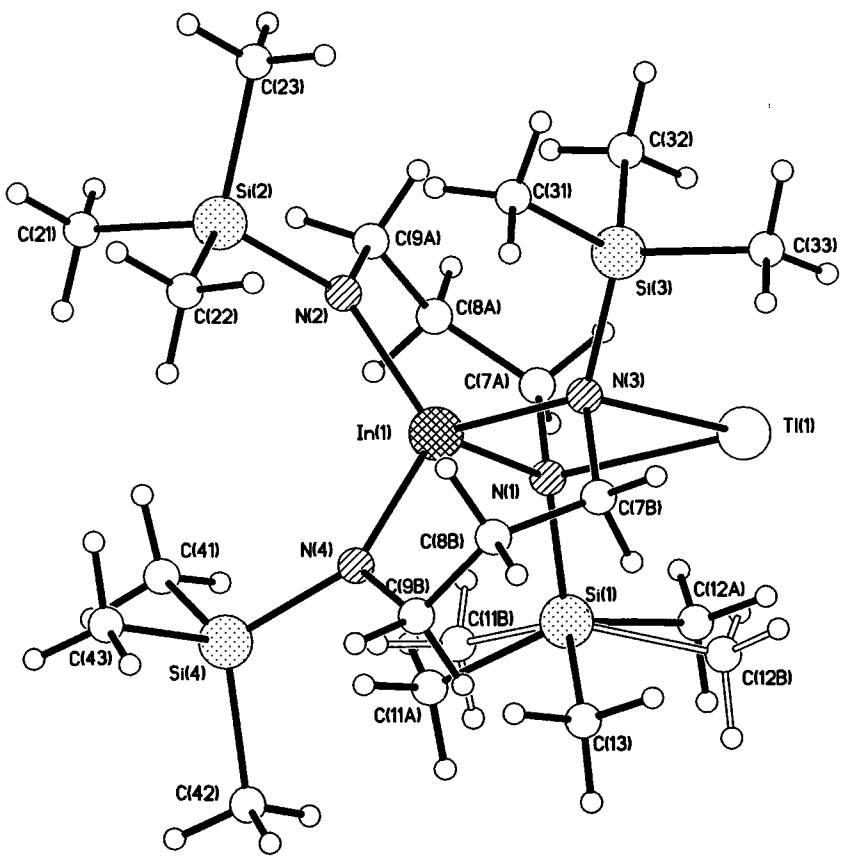

Fig. 3. Molecular structure of **7** ($In^{III}Tl^{I}$ isomer). Selected bond lengths (Å) and interbond angles (°) are shown in Table 2.

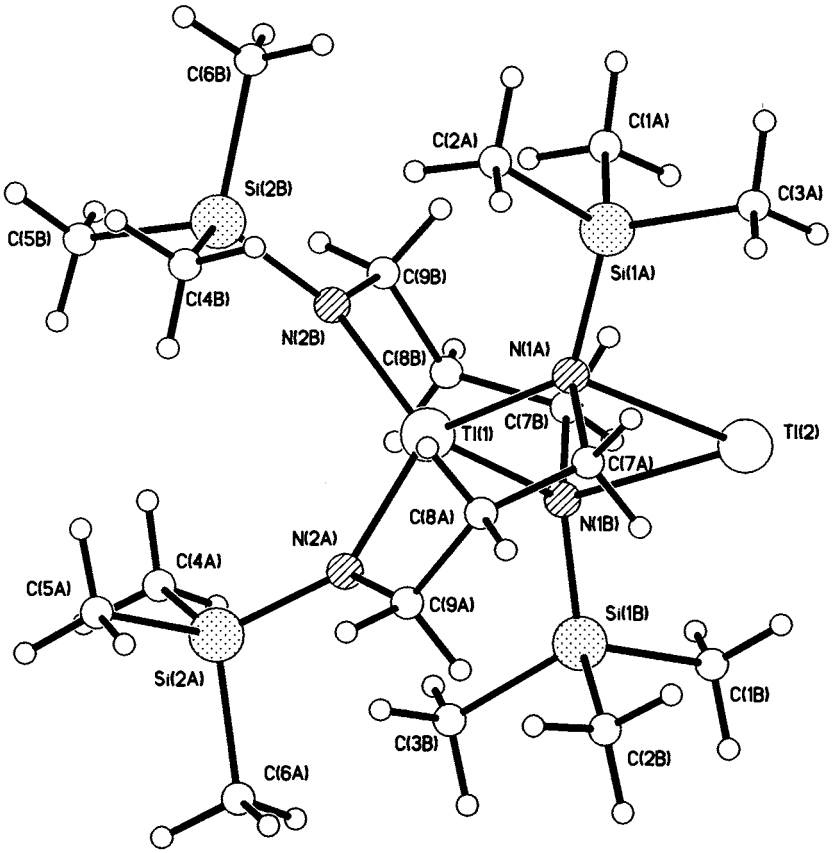

Fig. 4. Molecular structure of **8**. Selected bond lengths (Å) and interbond angles (°) are shown in Table 3.

In 25.92). ^{1}H-NMR (200.13 MHz, [d_6]-benzene, 295 K): δ 0.35 (s, 36 H, $Si(CH_3)_3$), 1.27 (m, 8 H, CH_2CH_2O), 1.73 (dm, $^{4}J_{TlH} = 43.1$ Hz, 4 H, CH_2CH_2N), 3.37 (m, 8 H, CH_2CH_2O), 3.49 (dm, $^{3}J_{TlH} = 316.2$ Hz, 8H, CH_2N). ^{7}Li-NMR (77.77 MHz, [d_6]-benzene, 295 K): δ 3.67. ^{29}Si-NMR (39.76 MHz, [d_6]-benzene, 295 K): δ 8.4 (d, $^{2}J_{TlSi} = 100.3$ Hz).

Table 2
Selected bond lengths (Å) and interbond angles (°) of **7**

Bond lengths (Å)			
In(1)–N(2)	2.027(14)	In(1)–N(4)	2.039(14)
In(1)–N(3)	2.207(14)	In(1)–N(1)	2.208(14)
In(1)–Tl(1)	3.481(2)	Tl(1)–N(1)	2.60(2)
Tl(1)–N(3)	2.601(14)	Si(1)–N(1)	1.753(14)
Si(2)–N(2)	1.75(2)	Si(3)–N(3)	1.749(14)
Si(4)–N(4)	1.75(2)		
Bond angles (°)			
N(2)–In(1)–N(3)	116.8(8)	N(4)–In(1)–N(3)	98.7(7)
N(2)–In(1)–N(1)	100.7(7)	N(4)–In(1)–N(1)	119.2(9)
N(3)–In(1)–N(1)	96.5(7)	N(1)–Tl(1)–N(3)	78.6(6).
		N(2)–In(1)–N(4)	122.7(8)

*3.3. Preparation of {[CH_2(CH_2NSiMe_3)$_2$]$_2$M}Tl (M = In **7**, Tl **8**)*

A solution of 898 mg (1.44 mmol) $CH_2[CH_2N(Tl)SiMe_3]_2$ in 20 ml THF was cooled to − 78°C and 33 mg (0.72 mmol) $InCl_3$ (for compound **7**) or 21 mg (0.72 mmol) $TlCl_3$ (for compound 8) was added while stirring. The mixture was allowed to react at r.t. for 3 h. After removal of the solvent the residue was extracted with 15 ml toluene and finally centrifuged. The centrifugate was concentrated to ca. 7 ml. After storing at − 30°C compound **6** was obtained as yellow, highly crystalline solid. Compound **7** was obtained by complete removal of toluene as yellow oil (12 h at high vacuum), which was crystallized at r.t. within 24 h.

Analytical data for compound **7**: Yield: 352 mg (65%), (found: C, 28.49; H, 6.35; N, 7.54; Tl, 27.21; In 15.34; $C_{18}H_{48}InN_4Si_4Tl$ calc.: C, 28.74; H, 6.43; N, 7.45; Tl 27.17; In 15.27). ^{1}H-NMR (200.13 MHz, [d_6]-benzene, 295 K): δ 0.29 (s, 36 H, $Si(CH_3)_3$), 1.73 (m, 4 H, CH_2CH_2N), 3.25 (m, 8 H, CH_2N). ^{13}C-NMR (50.32 MHz, [d_6]-benzene, 295 K): δ 3.2, 1.4 ($Si(CH_3)_3$), 39.7 (CH_2CH_2N), 49.3 (CH_2NN).

Analytical data for compound **8**: Yield: 448 mg (74%), (found: C, 25.54; H, 5.85; N, 6.82; Tl, 31.67;

Table 3
Selected bond lengths (Å) and interbond angles (°) of **8**

Bond lengths (Å)			
Tl(1)–N(2A)	2.11(3)	Tl(1)–N(2B)	2.12(2)
Tl(1)–N(1A)	2.22(3)	Tl(1)–N(1B)	2.24(3)
Tl(1)–Tl(2)	3.514(3)	Tl(2)–N(1B)	2.53(3)
Tl(2)–N(1A)	2.54(3)		
Bond angles (°)			
N(2A)–Tl(1)–N(2B)	124(2)	N(2A)–Tl(1)–N(1A)	102.7(12)
N(2B)–Tl(1)–N(1A)	118(2)	N(2A)–Tl(1)–N(1B)	115.2(13)
N(2B)–Tl(1)–N(1B)	100.8(11)	N(1A)–Tl(1)–N(1B)	91.8(12).

$C_{18}H_{48}N_4Si_4Tl_2$ calc.: C, 25.69; H, 5.75; N, 6.66; Tl 31.72;). ^{1}H-NMR (200.13 MHz, C_6D_6, 295 K): δ 0.28 (s, 36 H, $Si(CH_3)_3$), 1.73 (dquin, 4 H, $^4J_{TlH} = 42.1$ Hz, CH_2CH_2N), 3.42 (dm, 8 H, $^3J_{Tl} = 317.9$ Hz, CH_2N). ^{29}Si-NMR (39.76 MHz, C_6D_6, 295 K): 8.2 (d, $^2J_{TlSi} = 237.9$ Hz), 9.1 (br s).

3.4. X-ray crystallographic studies of **2**, **7** and **8**

Data were collected using a Siemens P4 diffractometer at a temperature of 293 K with crystals mounted in Lindemann capillaries under argon. Crystal data and experimental details for the crystals of **2**, **7** and 8 are given in Table 4. Crystals of **7** and **8** diffracted very weakly and both showed evidence of some disorder. Despite resultant relatively high S.D. on all parameters of **7** and **8**, the main structural features of these unusual molecules are well established. In the case of **7** the most satisfactory refinement is achieved with random replacement of 13% of the molecules of **7** by an isomer in which thallium and indium positions are interchanged, so that in the model refined the light atoms from the two components were effectively superimposed; rotational disorder of the trimethylsilyl groups was indicated by the relatively high displacement parameters, and this was partially resolved for one group. For the structure of **8** unresolved disorder was indicated by high thermal displacement parameters for the peripheral trimethylsilyl groups and *exo*-thallium. In both structures chemically equivalent bond lengths were restrained to be equal within experimental error. In the final cycles of refinement all non-hydrogen atoms of **2** and **7** (apart from the four carbon sites of partial occupancy) and the thallium and silicon atoms of **8** were assigned anisotropic displacement parameters. Hydrogen atoms were included in idealized positions riding on the parent atoms and were assigned isotropic displacement parameters of 1.2 U_{eq} of the parent atom for methylene groups and 1.5 U_{eq} for methyl groups.

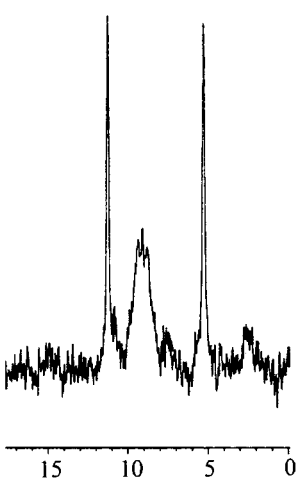

Fig. 5. ^{29}Si-NMR spectrum of **8** recorded in toluene-d_8 at 220 K and displaying $^{203/205}$Tl-^{29}Si-coupling.

Acknowledgements

This work was funded by the Deutsche Forschungsgemeinschaft, the Fonds der Chemischen Industrie, the Engineering and Physical Science Research Council, the Deutscher Akademischer Austauschdienst and the British Council (ARC grant to L.H. Gade and M. McPartlin).

Table 4
Crystal data and structure refinement for **8**

Empirical formula	$C_{18}H_{48}N_4Si_4TI_2$
Formula weight	841.70
Temperature	298(2) K
Wavelength	0.71073 Å
Crystal system	Orthorhombic
Space group	$P2_1$
Unit cell dimensions	$a = 21.179(3)$ Å
	$b = 10.3403(12)$ Å
	$c = 14.487(2)$ Å
Volume, Z	3172.7(7) Å^3, 4
$D_{calc.}$	1.762 mg m^{-3}
Absorption coefficient	10.307 mm^{-1}
$F(000)$	1608
Crystal size	$0.32 \times 0.48 \times 0.48 \times$ mm
θ range for data collection	1.92 to 20.99
Limiting indices	$-1 \le h \le 21$, $-1 \le k \le 10$,
	$-1 \le l \le 14$
Reflections collected	2381
Independent reflections	1963 ($R_{int} = 0.0804$)
Refinement method	Full-matrix least-squares on F^2
Data/restraints/parameters	1961/51/143
Goodness-of-fit on F^2	1.053
Final R indices [$I > 2\sigma(I)$]	$R_1 = 0.0698$, $wR_2 = 0.1181$
R indices (all data)	$R_1 = 0.1524$, $wR_2 = 0.1509$
Absolute structure parameter	0.04(3)
Largest diff. peak and hole	1.013 and -1.075 e Å^{-3}

References

[1] (a) W. Uhl, Angew. Chem. 105 (1993) 1449. (b) Angew. Chem. Int. Ed. Engl. 32 (1993) 1386.
[2] (a) K.W. Hellmann, L.H. Gade, A. Steiner, D. Stalke, F. Möller, Angew. Chem. 109 (1997) 99. (b) K.W. Hellmann, L.H. Gade, A. Steiner, D. Stalke, F. Möller, Angew. Chem. Int. Ed. Engl. 36 (1997) 160.
[3] (a) K.W. Hellmann, L.H. Gade, I.J. Scowen, M. McPartlin, Chem. Commun. (1996) 2515. (b) K.W. Hellmann, L.H. Gade, R. Fleischer, T. Kottke, Chem. Eur. J. 3 (1997) 1801. (c) K.W. Hellmann, C.H. Galka, L.H. Gade, A. Steiner, D.S. Wright, T. Kottke, D. Stalke, Chem. Commun. (1998) 549.
[4] K.W. Hellmann, L.H. Gade, R. Fleischer, D. Stalke, Chem. Commun. (1997) 527.
[5] Reviews: (a) Unkonventionelle Wechselwirkungen in: B. Krebs (Ed.), der Chemie Metallischer Elemente, VCH, Weinheim, 1992. (b) P. Pyykkö, Chem. Rev. 97 (1997) 597. (c) Theoretical work: C. Janiak, R. Hoffmann, J. Am. Chem. Soc. 112 (1990) 5024. (d) G. Treboux, J.-C. Barthelat, J. Am. Chem. Soc. 115 (1993) 4870. (e) P. Schwerdtfeger, Inorg. Chem. 30 (1991) 1660 and refs. cited.
[6] (a) M. Veith, A. Spaniol, J. Pöhlmann, F. Gross, V. Huch, Chem. Ber. 126 (1993) 2625. (b) K.W. Klinkhammer, S. Henkel, J. Organomet. Chem. 480 (1994) 167 and refs. cited therein.
[7] S. Friedrich, L.H. Gade, I.J. Scowen, M. McPartlin, Organometallics 14 (1995) 5344.
[8] S. Friedrich, L.H. Gade, I.J. Scowen, M. McPartlin, Angew. Chem. 108 (1996) 1440. (b) S. Friedrich, L.H. Gade, I.J. Scowen, M. McPartlin, Angew. Chem. Int. Ed. Engl. 35 (1996) 1338.
[9] D.J. Brauer, H. Bürger, G.R. Liewald, J. Organomet. Chem. 308 (1986) 119.
[10] M.G. Gardiner, C.L. Raston, Inorg. Chem. 34 (1995) 4206.
[11] K. Gregory, P.V.R. Schleyer, R. Snaith, Adv. Inorg. Chem. 37 (1991) 47.
[12] (a) M. Veith, M. Zimmer, S. Müller-Becker, Angew. Chem. 37 (1993) 1771. (b) Angew. Chem. Int. Ed. Engl. 32 (1993) 1771.
[13] H. Friebolin, Ein- und Zweidimensionale NMR-Spektroskopie, 2nd ed., VCH, Weinheim, 1992.
[14] K.W. Hellmann, L.H. Gade, Verfahrenstechnik 31 (5) (1997) 70.